SYNTHESIS AND RECONSTRUCTION OF FUNCTIONS SATISFYING SIMULTANEOUS TIME AND FREQUENCY DOMAIN CONSTRAINTS USING ALTERNATING CONVEX PROJECTIONS WITH OVERRELAXATION: AN APPLICATION IN IMAGE DESIGN

By

Hong, Joo Heng

A THESIS

Submitted to
Michigan State University
in partial fulfillment of the requirements
for the degree of

MASTER OF SCIENCE

Department of Electrical Engineering
and System Science

1985

ACKNOWLEDGEMENT

I wish to express my sincere gratitude to Professor Soheil I. Sayegh for his expert guidance and stimulating advice throughout the course of this research. This research could not have been accomplished without his encouragement and support. I would like to thank my father and my mother whose support and love have encouraged me to make this thesis possible.

TABLE OF CONTENTS

Chapter		Page
1	INTRODUCTION	1
2	MATHEMATICAL FORMULATION	6
	2.1 General algorithm description	6
	2.2 Mathematical formulation for imaging system ...	9
	2.3 Incoherent case	9
	2.3.1 Sets and Projection operators	10
	2.4 Coherent case	14
	2.4.1 Sets and Projection operators	15
3	RESULTS AND DESCRIPTION	20
	3.1 Parameters specification	20
	3.2 Description of image synthesis results	22
	3.3 Numerical results for the phase restoration of an 1-D bandlimited function	23
4	CONCLUSIONS, DISCUSSIONS AND FURTHER RESEARCH	26
APPENDIX A	....	28
APPENDIX B	....	30
APPENDIX C	....	36
FIGURES	....	51
REFERENCES	....	68

ABSTRACT

SYNTHESIS AND RECONSTRUCTION OF FUNCTIONS SATISFYING SIMULTANEOUS TIME AND FREQUENCY DOMAIN CONSTRAINTS USING ALTERNATING CONVEX PROJECTIONS WITH OVERRELAXATION: AN APPLICATION IN IMAGE DESIGN

By

Hong, Joo Heng

A method of alternating projections with overrelaxation is employed for synthesizing images that are band-limited in the frequency domain and with predetermined threshold crossings in the space domain. This problem is encountered when we want to generate a prescribed binary image at the output of a diffraction-limited imaging system with high contrast recording. Such an imaging system is modeled as a linear band-limited system followed by a noninvertible point nonlinearity. Some of the important applications of image synthesis are the construction of masks for microlithography, laser printing, fabrication of surface acoustic wave devices and the storage of data using optical techniques. With a suitable choice of the overrelaxation parameter for the algorithm, it is found that the number of iterations required for this method is several orders of magnitude smaller than that required for the Gerchberg-Papoulis type algorithm. This improvement is very important in designing images that are much more complex and of practical interest. Both incoherent imaging and coherent imaging systems are investigated.

CHAPTER 1

INTRODUCTION

There are many problems of great interest in science and engineering where one wishes to reconstruct or synthesize functions which are specified partially in the time (or space) domain and partially in the frequency domain (Fourier domain). The task of finding functions satisfying such simultaneous constraints is a difficult one and depends on the constraints themselves. The problem however is very important as it arises in numerous situations.

An example is the extrapolation of band-limited functions where only a finite segment of a band-limited function is given and it is desired to find the value of the function everywhere [8]. Another example is the recovery of a real nonnegative signal from the knowledge of the magnitude only of its Fourier Transform. Such a problem arises in X-ray crystallography, Fourier Transform spectroscopy and imaging through atmospheric turbulence using interferometer data [9]. Still some other problems dealing with certain constraints are blind deconvolution [10], computer holography [11], kinoforms [12], design of radar signals, antenna arrays [13] and digital filters [14].

One may divide the problems of searching for functions satisfying simultaneous time and frequency domain constrains into two classes :

restoration and synthesis problems. In restoration problems, one wants to reconstruct a function (or a close replica of it) given that the function satisfies certain constraints. By the very nature of the problem, a solution must exist. In the synthesis problems, one wants to construct a function satisfying some specified constraints. A solution, however, may or may not exist. For example, one cannot construct a function that is of finite time extent and, at the same time, of finite frequency extent. Another important point is the question of uniqueness of the solution. If a whole class of functions satisfies the given constraints in a restoration problem, we have to determine which function within the class is the solution. In the synthesis problem, on the other hand, one may be interested only in finding a solution. For example, when designing filters with certain time and frequency domain specifications, the primary concern is in finding some function satisfying all the given requirements. Later one may (or may not) choose to seek an 'optimum' choice. Therefore the uniqueness question is of more concern in restoration problems than in synthesis problems.

In this thesis, I deal with the problem of 'synthesis of images through a diffraction-limited imaging system with high contrast recording'. This is to generate a prescribed binary image at the output of an imaging system. Some important applications of this image synthesis problem are the design of masks for microlithography, the fabrication of surface acoustic wave devices, the storage of data using optical techniques, laser printing and so forth.

The models for the imaging system I will deal with are shown in Figure 2.1 and Figure 2.2 for the incoherent and coherent system respectively. These are adequate models for a microphotographic system where the linear system represents a diffraction-limited microcamera operating near its resolution limit and the noninvertible hard-limiter represents a very high contrast recording film [5]. In mathematical terms, the output $\tilde{g}$ must be band-limited and after passing through the nonlinear device (noninvertible hard-limiter), will produce a binary image according to the white (black) regions of the binary desired image g that we want to construct. In other words, the overall purpose of the image synthesis problem is to synthesize $\tilde{g}$ such that it satisfies the Fourier domain constraint which is band-limited and the space domain constraint corresponding to predetermined threshold crossings.

Some ad hoc methods for the solution of this image construction problem have been proposed [3,4]. An example is corrections being deliberately introduced in the original masks to compensate for the distortions caused by the microcamera itself. More recently, it was shown that this problem can be reduced to a linear programming problem which can be solved by using well known techniques [6,7]. Although the linear programming approach is superior to the ad hoc technique proposed earlier, it still suffers from the heavy amount of computation required, which prohibits its use on real images except for some very simple patterns. Another method for finding the solution is a variation of the Gerchberg-Papoulis algorithm (also refered to as the

Gerchberg-Saxton algorithm) [1]. The algorithm itself is an iterative one, with an initial guess for the solution consistent with the given information (constraint) in one domain, repeated transformations are performed between the space domain and the frequency domain. In each domain, the known information (contraints) is incorporated into the current estimate of the desired function (solution), forcing the estimate to satisfy the constraints corresponding to the information specified in both domains. Depending upon the constraints themselves, the algorithm may converge or fail to converge at all.

The method presented in this thesis is the method of alternating projections with overrelaxation over closed convex sets in Hilbert space [2]. The concept is that the function f which we want to synthesize is belonging to the intersection C_0 of m well-defined closed convex sets C_i's, $i=1 \rightarrow m$. That is , the known properties (given information or constraints) of the function f form m well-defined closed convex sets C_i's, $i=1 \rightarrow m$, and such that

$$f \varepsilon C_0 = \bigcap_{i=1}^{m} C_i .$$

Note that the intersection C_0 is also a closed convex set containing f. If the desired function f does satisfy the above constraints, then the problem of synthesizing f from its m properties is included in that of finding at least one point (one function) belonging to C_0.

In chapter 2, both the incoherent and coherent models for the imaging system mentioned previously and the known properties (constraints) corresponding to the closed convex sets of the function which we want to construct are mathematically formulated. The algorithm for finding the fixed point (solution) belonging to the intersection C_0 which is closed and convex of the image design problem will be considered in great detail.

In chapter 3, some examples of 2-dimensional patterns that were designed using the algorithm presented in chapter 2 are presented. A comparison based on convergence rate is made between this algorithm and the Gerchberg-Papoulis type algorithm presented in [1]. Besides, numerical results of an 1-dimensional example for reconstructing the phase of a band-limited function using the method proposed in chapter 2 are also presented. In chapter 4, some discussions and suggestions are made for the image design problems in the future.

CHAPTER 2

MATHEMATICAL FORMULATION

2.1 General algorithm description

The image synthesis problem is closely related to the well known problem of image restoration. The main difference between these two problems is the existence of a solution. In image restoration, by the very nature of the problem, a solution must exist. While in the image synthesis problem, the solution does not necessary exist. An example is that one cannot synthesize a function that is time-limited as well as band-limited.

In the image restoration problem, the observed properties of the output function restrict the input function f to have certain properties (given information or constraints). If every known property of the input function f form a well-defined closed convex set C_i, i=1→m, in Hilbert space H, then m such properties place f in the intersection

$$C_0 = \bigcap_{i=1}^{m} C_i$$

of the corresponding closed convex sets $C_1, C2, \ldots C_m$. The intersection C_0 is also closed and convex and contains f. Consequently, irrespective of whether C_0 contains elements other than f, the problem of restoring the function f from its m properties is included in that of finding at least one point (one function) belonging to C_0. Therefore, if the operator P_0 projecting onto C_0 is known, the problem is solved, for then $P_0x\varepsilon C_0$ for every $x\varepsilon H$. However, C_0 in general can be considerably more complex in structure than any of the C_i's corresponding to the constraints and a direct realization of P_0 is usually not feasible.

An alternate approach [2] for solving the problem is to consider every known property of the function f that places it in a well-defined closed convex subset, and search for the intersection. If the projection operators P_i's on its respective C_i's, i.e., $P_ix\varepsilon C_i$, for $x\varepsilon H$ and $P_ix=x$ for $x\varepsilon C_i$, is effectively realizable, $i=1\to m$, then to find a point (function) satisfying the m given properties, a composition operator T will be defined as follows:

$$T=P_mP_{m-1}P_{m-2}\cdots\cdot P_1.$$

The operator T is in general not the projection operator onto C_0, but every point of C_0 is a fixed point for every P_i and therefore of T, i.e., if $x\varepsilon C_0$, then $x\varepsilon C_i$, $P_ix=x$, $i=1\to m$ and $Tx=x$. With the initial guess other than the points belonging to C_0, the iterative scheme has been developed for the generation of fixed points of T by the standard recursion

$X_{n+1}=T^nX$, where

X : the arbitrary initial guess,

n : the number of iterations.

It has been shown that [2] a nonexpansive mapping $T:H \to H$ of a Hilbert space onto itself is a reasonable wanderer and, a fortiori, asymptotically regular, and the sequence $\{T_n x\}$ converges weakly to a fixed point of T. However, if the Hilbert space is of finite dimension, the sequence $\{T_n x\}$ will converge strongly to $P_0 x$ for every $x \in H$.

What is needed then is to define nonexpansive projection operators P_i's, $i=1 \to m$, on the the respective C_i's, for a composition of two or more nonexpansive mappings is also nonexpansive.

Lemma 1 [16] [17] : Let C denote any closed convex subset of Hilbert space H, then there exists a unique $g \in C$ such that

$$\inf_{x \in C} \|f-x\| = \|f-g\| .$$

Now, the projection operator P_i onto C_i is defined as follows:

$$\|f-P_i f\| = \min_{x \in C_i} \|f-x\|.$$

That is, the projection assigns to every $f \in H$ its nearest neighbor $P_i f$ in C_i. This defines a nonlinear projection operator $P_i:H \to C_i$ unambiguously by means of the minimality criterion.

The projection operators P_i's, $i=1 \to m$, defined above can be shown to be nonexpansive and continuous [2]. However the convergence rate using the composition of these operators is not at a geometric rate.

The convergence can be speeded up considerably if we replace P_i by $T_i=1+\xi_i(P_i-1)$, $\xi_i=1\to 2$ (overrelaxation) with a proper choice of the ξ_i [2]. It can also be shown that [2] the operators T_i's are nonexpansive.

2.2 Mathematical formulation for the imaging system

Image construction involves determing the object distribution which produces a prescribed image at the output of a given imaging system. The imaging system I deal with in this thesis is a diffraction-limited imaging system with a high contrast recording device. Such an imaging system is modeled as a linear band-limited system followed by a hard-limiting point nonlinearity (clipper).

The overall system is mathematically represented by the operator G, where the input and the output image f and g, are related by g=Gf. The system G is known and a prescribed image g is to be generated at the output of the system.

2.3 Incoherent case

The mathematical model for an incoherent diffraction-limited imaging system with high contrast recording device is shown in Figure 2.1. This is an adequate model for a microphotographic system where the linear system represents a diffraction-limited microcamera operating near its resolution limit and the hard-limiter represents a very high contrast film [5]. The input function represents the intensity distribution which is a nonnegative valued function.

Referring to this figure, we note that the value of g (intensity distribution) will be equal to 1 whenever $\tilde{g}$ is above the threshold γ and will be equal 0 when $\tilde{g}$ is below γ. The value of γ is determined by the recording material characteristics. Because practical systems are not expected to exhibit the infinitely sharp characteristics of the hard-limiter shown in Figure 2.1, a forbidden zone $(-\varepsilon,\varepsilon)$ has been introduced about the threshold. Without loss of generality, we shall take γ to be equal to zero since the threshold can be adjusted without affecting g by simply introducing a dc bias in the input function f.

2.3.1 Sets (constraints or known properties) and projection operators

1] C_1: The subset of all functions band-limited to b rads/s, i.e., $f \in C_1$ iff $F(\omega)=0$ almost everywhere (a.e.) in $|\omega|>b$. It is obvious that C_1 is a closed convex set devoid of interior points. Given an arbitrary $f \in H$, its projection onto C_1 is realized by

$$P_1 f \xleftrightarrow{\mathcal{F}} P_b(\omega)F(\omega) \quad \text{,where}$$

$$P_b(\omega)=\begin{cases} 1, & |\omega|\leq b, \\ 0, & |\omega|>b, \end{cases}$$

$$f \xleftrightarrow{\mathcal{F}} F(\omega).$$

2] C_2: The subset of all functions with predetermined threshold crossings and being the same as those of the desired given function and the absolute value is greater than ε. To demonstrate closure of this set we must show that given a sequence $\{f_n\}$ with limit f (written $f_n \to f$) that $\{f_n\} \varepsilon C_2$ implies $f \varepsilon C_2$.

Let f be the limit of the sequence $\{f_n\}$, then we can write

$$\iint |f_n - f|^2 dxdy \to 0.$$

This requires that f have the same threshold crossing as those of the desired given function g and the absolute value be greater than ε, and C_2 be closed as claimed. The set is also convex, for f_1 and $f_2 \varepsilon C_2$, $\mu f_1 + (1-\mu) f_2 \varepsilon C_2$ for $0<\mu<1$. Therefore, C_2 defined as above is a closed convex set. The projection onto this set is

$$P_2f(x)=\begin{cases} f(x), & f(x) \text{ has same sign as } g(x) \text{ and } |f|>\varepsilon \\ \text{sign}(g(x))\varepsilon, & f(x) \text{ is of different sign as } g(x) \\ & ;\text{or } |f|<\varepsilon, \end{cases}$$

where $g(x)$ is the desired given function. The values of g will be negative if it is below the threshold (which is equal to 0 here) and will be positive if it is above the threshold.

Since the algorithm will be implemented on a digital computer, all the functions mentioned above will be described in discrete form (the discretization is done using a square grid with N points). The algorithm will be implemented as follows:

$$P_1[f(m,n)]=\left[W^{-1}B_TW\right]f(m,n),$$

where

$$W[f(m,n)]=F(k,l)=\sum_{m=0}^{N-1}\sum_{n=0}^{N-1}e^{-j2\pi mk/N}e^{-j2\pi nl/N}$$

is the two-dimensional (cartesian) discrete Fourier Transform (2-D DFT) of the sequence $\{f(m,n)\}$, W^{-1} is the inverse 2-D DFT, and

$$B_T[F(k,l)]=F(k,l).H(k,l),$$

where $H(k,l)$ is an ideal low-pass filter in frequency domain taking values zero and one only. Using overrelaxation, we form the function

$$f'(m,n)=(1-\xi_1)f(m,n)+\xi_1 P_1[f(m,n)]=T_1[f(m,n)].$$

Then,

$$P_2[f'(m,n)]=\begin{cases} f'(m,n), & f'(m,n).g(m,n) \text{ is positive and } |f'(m,n)|\geq\varepsilon \\ g(m,n)\varepsilon, & f'(m,n).g(m,n) \text{ is negative or } |f'(m,n)|<\varepsilon \end{cases}$$

Using overrelaxation again, we form the function

$$f_1(m,n)=(1-\xi_2)f'(m,n)+\xi_2 P_2[f'(m,n)]=T_2[f'(m,n)].$$

Note, the desired function $g(m,n)$ takes the values -1 and +1 only for the white and black region respectively. The n^{th} iteration is realized as follows:

$$f_n(m,n)=T[f_{n-1}(m,n)=T^n[f(m,n)],$$

where

$f(m,n)$ is the initial guess,

$T=T_1T_2$,

$T_1=1+\xi_1(P_1-1)=(1-\xi_1)+\xi_1P_1$,

$T_2=1+\xi_2(P_2-1)=(1-\xi_2)+\xi_2P_2$.

2.4 Coherent case

The mathematical model for a coherent diffration-limited imaging system is shown in Figure 2.2. The input function f represents the field distribution instead of the intensity distribution as in the incoherent case. In mathematical terms, the square of the magnitude of the bandlimited field distribution $\tilde{g}$ at each point is above (below) a fixed threshold γ according to the white (black) regions of the desired binary pattern g. ε has been introduced about the threshold for the same purpose as the incoherent case mentioned earlier.

Note that the set of input functions can include complex functions in this case. By extending the class of inputs to include complex functions as well, we hope to have better resolution. However, the algorithm proposed here is dealing with projections onto convex sets. If the class of input is allowed to include complex functions as well, the restriction on $|\tilde{g}|$ will lead us to a nonconvex set, a problem that the algorithm presented above cannot handle. Therefore, for the time being, it is necesary for us to restrict ourselves to the set of real functions. The problem involving nonconvex sets will be discussed in more detail in chapter 4. Furthermore, some numerical results for restoring the phase of a complex band-limited function will also be presented in the Bnext chapter, where the restrictions are nonconvex.

2.4.1 Sets and projection operators

1] C_1 : The subset of all functions band-limited to b rad/s, which is the same as that defined in the incoherent case. Given the arbitrary $f \in H$, its projection onto C_1 is realized as that of before, i.e.,

$$P_1 f \overset{\mathcal{F}}{\longleftrightarrow} P_b(\omega)F(\omega),$$

where

$$P_b(\omega) = \begin{cases} 1, & |\omega| \leq b \\ 0, & |\omega| > b \end{cases}$$

$$f \overset{\mathcal{F}}{\longleftrightarrow} F(\omega).$$

2] C_2: The subset of all functions whose square magnitude will have the predetermined threshold crossings and being the same as those of the desired given image and does not fall in the region $(\gamma-\varepsilon,\gamma+\varepsilon)$. For the purpose of convexity, the negative values of the function will never be smaller than $-(\gamma-\varepsilon)^{1/2}$. Since, refering to the figure shown below, if the negative values are allowed to be smaller than $-(\gamma-\varepsilon)^{1/2}$, then for two points, say x_1 and x_2 where x_2 is negative, the magnitude square for these two points is above the threshold. However $\mu x_1+(1-\mu)x_2$, for $0<\mu<1$, will fall in the region $\{-(\gamma)^{1/2},(\gamma)^{1/2}\}$, where the magnitude square is below threshold, and violate the convexity. As in the incoherent case, this set also can be shown to be closed.

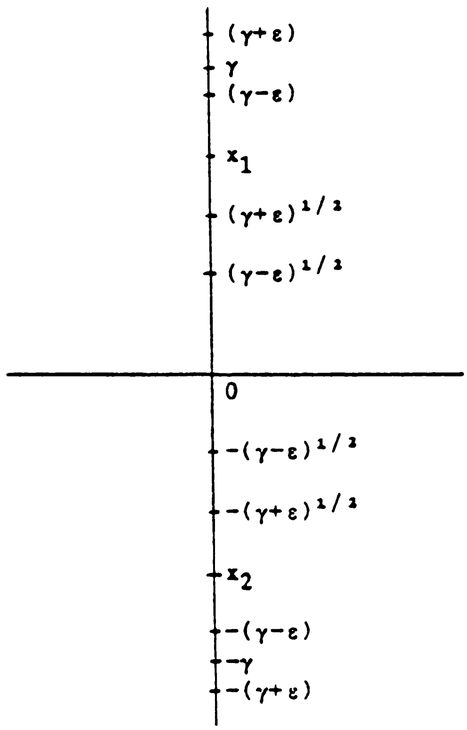

Figure 1.

The projection operator P_2 on this set is defined as

$$P_2[f(x)]=\begin{cases} f(x), & |f(x)|\leq(\gamma-\varepsilon)^{1/2} \text{ and } |g(x)|\leq(\gamma-\varepsilon)^{1/2} \\ f(x), & f(x)>(\gamma+\varepsilon)^{1/2} \text{ and } |g(x)|\geq(\gamma+\varepsilon)^{1/2} \\ (\gamma+\varepsilon)^{1/2}, & |g(x)|\geq(\gamma+\varepsilon)^{1/2} \text{ and } f(x)<(\gamma+\varepsilon)^{1/2} \\ (\gamma-\varepsilon)^{1/2}, & |g(x)|\leq(\gamma-\varepsilon)^{1/2} \text{ and } f(x)\geq(\gamma-\varepsilon)^{1/2} \\ -(\gamma-\varepsilon)^{1/2}, & |g(x)|\leq(\gamma-\varepsilon)^{1/2} \text{ and } f(x)<-(\gamma-\varepsilon)^{1/2} \end{cases}$$

where $g(x)$ is the desired given function and γ is the threshold value.

In discrete-time form, the algorithm is implemented as follows:

$$P_1[f(m,n)=\left[W^{-1}B_TW\right]f(m,n)$$

where

$$W[f(m,n)]=F(k,l)=\sum_{m=0}^{N-1}\sum_{n=0}^{N-1}f(m,n)e^{-j2\pi mk/N}e^{-j2\pi nl/N}$$

is the 2-D DFT of the sequence $\{f(m,n)\}$, W^{-1} is the 2-D DFT, and

$$B_T[F(k,l)]=F(k,l).H(k,l),$$

where $H(k,l)$ is an ideal low-pass filter in frequency domain taking values zero and one only. Using overrelaxation, we form the function

$$f'(m,n)=(1-\xi_1)f(m,n)+\xi_1 P_1[f(m,n)]=T_1[f(m,n)].$$

Then,

$$P_2[f(m,n)]=\begin{cases} f'(m,n), & g(m,n)=0 \text{ and } |f'(m,n)| \le (\gamma-\varepsilon)^{1/2} \\ f'(m,n), & g(m,n)=1 \text{ and } |f'(m,n)| \ge (\gamma+\varepsilon)^{1/2} \\ (\gamma+\varepsilon)^{1/2}, & g(m,n)=1 \text{ and } |f'(m,n)z| \le (\gamma+\varepsilon)^{1/2} \\ (\gamma-\varepsilon)^{1/2}, & g(m,n)=0 \text{ and } f'(m,n) \ge (\gamma-\varepsilon)^{1/2} \\ -(\gamma-\varepsilon)^{1/2}, & g(m,n)=0 \text{ and } f'(m,n) \le -(\gamma-\varepsilon)^{1/2} \end{cases}$$

where $g(m,n)$, the desired output function, takes the values 0 and 1 only corresponding to the white and black regions respectively of the desired given function, and γ is the threshold value. Using overrelaxation, we form the function

$$f_1(m,n)=(1-\xi_2)f'(m,n)+\xi_2 P_2[f'(m,n)]$$
$$=T_2[f'(m,n)].$$

The n^{th} iteration step proceeds as follows:

$$f_n=T[f_{n-1}(m,n)]=T^n[f(m,n)],$$

where

$f(m,n)$ is the initial guess,

$$T=T_1 T_2$$

$$T_1=1+\xi_1(P_1-1)=(1-\xi_1)+\xi_1 P_1$$

$$T_2=1+\xi_2(P_2-1)=(1-\xi_2)+\xi_2 P_2.$$

CHAPTER 3

RESULTS AND DESCRIPTIONS

Five two-dimensional patterns were designed for the incoherent imaging system using the algorithm presented in this thesis.

3.1 Parameters specification

The parameters listed below are needed to specify the images and the algorithm.

N: The number of pixels sampled on the pattern along each dimension.

M: $\log_2 N$

LWP: The bandwidth of the low pass filter along each dimension corresponding to the diffraction-limited microcamera.

ξ_i: The overrelaxation constant for the algorithm.

ε: The value for the forbidden zone about the threshold.

The values of the parameters for the program (Appendix C) implemented on the PRIME 750 digital computer are as follows:

For patterns 1, 2 and 3

$N=32$

$M=5$

$\xi_1=\xi_2=1.995$

$\varepsilon=0.001$

$$LWP=\begin{cases} 6 & \text{;for pattern 1} \\ 11 & \text{;for pattern 2} \\ 11 & \text{;for pattern 3.} \end{cases}$$

For patterns 4 and 5

$N=64$

$M=6$

$\xi_1=\xi_2=1.995$

$\varepsilon=0.001$

$$LWP=\begin{cases} 17 & \text{;for pattern 4} \\ 26 & \text{;for pattern 5} \end{cases}$$

3.2 Description of image synthesis results

Figure 3a represents the desired image which we want to construct at the output of the imaging system of Figure 2.1. If we feed this image to the input of the imaging system, the output from the clipper will be as shown in Figure 3b. Clearly, it is highly distorded by the imaging system and therefore the straightforward approach consisting of using the desired pattern itself as an input is not appropriate.

Using the algorithm proposed in this thesis, I succeeded in finding the solution (required input image) that will produce an exact replica of the desired pattern after passing through the imaging system. The value of the solution (required input image) is then quantized into 10 gray levels and shown in Figure 3c. Figure 4 to Figure 7 are presented in the same format as Figure 3.

The number of iterations required to find the solutions for each of the images are listed below in Table 1. In addition, the number of iterations required for the Gerchberg-Papoulis algorithm [1] is also included. It can be seen that the algorithm presented here gives great improvements over the Gerchberg-Papoulis algorithm.

3.3 Numerical results for the phase restoration of an 1-D bandlimited function

The numerical results presented in Table 2 represent the sum of square error when I try to use the algorithm presented here to recover the phase in the time domain of a one-dimensional band-limited function. The magnitude and phase of the function are known a priori. The phase of the function is then thrown away and the function goes through the algorithm with initial random phase and the original known magnitude. It is found that, for the 1-D case, the sum of square error is very small after a certain number of iterations, even though the phase restoration leads to a nonconvex projection problem.

Tabble 1

Number of iterations to reach convergence

	Convex projections with overrelaxation	Gerchberg-Papoulis algorithm [1]
Pattern 1	19	414
Pattern 2	14	216
Pattern 3	20	613
Pattern 4	13	**
Pattern 5	80	**

Table 2

(The values presented below represent the sum of square error of recovering the phase of an 1-D bandlimited function with N=128)

<u>LWP=28</u>

The value for ξ

		1.50	1.70	1.74
	0	110.86	110.86	110.86
	10	2.672	2.62	2.61
	50	0.645	0.358	0.47
no. of iterations	100	0.296	7.68×10^{-2}	0.138
	150	0.173	5.10×10^{-2}	7.90×10^{-2}
	200	0.116	4.20×10^{-2}	7.38×10^{-2}
	250	7.39×10^{-2}	4.09×10^{-2}	6.99×10^{-2}
	299	4.75×10^{-2}	4.03×10^{-2}	7.07×10^{-2}

Table 2 (continue)

<u>LWP=30</u>

The value for ξ

no. of iterations	1.75	1.84	1.85
0	115.93	115.92	115.92
10	3.502	3.880	3.939
50	1.485	0.816	0.971
100	7.34×10^{-2}	8.00×10^{-3}	8.96×10^{-2}
150	2.70×10^{-2}	2.56×10^{-4}	8.95×10^{-2}
200	1.35×10^{-2}	7.57×10^{-5}	8.95×10^{-2}
250	8.82×10^{-3}	3.21×10^{-5}	8.95×10^{-2}
299	6.37×10^{-3}	1.64×10^{-5}	8.13×10^{-2}

<u>LWP=34</u>

The value for ξ

no. of iterations	1.85	1.865	1.87
0	119.847	119.847	119.947
10	1.105	1.110	1.113
50	1.18×10^{-2}	1.09×10^{-2}	5.18×10^{-2}
100	4.27×10^{-3}	1.69×10^{-2}	7.32×10^{-2}
150	1.19×10^{-3}	1.16×10^{-3}	7.52×10^{-2}
200	1.12×10^{-3}	1.12×10^{-3}	5.66×10^{-2}
250	1.10×10^{-3}	1.09×10^{-3}	7.47×10^{-2}
299	1.07×10^{-3}	1.07×10^{-3}	5.58×10^{-2}

CHAPTER 4

CONCLUSIONS, DISCUSSIONS AND FURTHER RESEARCH

By using the alternating projections method and appropriately defining the closed convex sets corresponding to the constraints of the functions which we want to construct, we can find a solution whenever the solution exists. Furthermore, with the particular choice of $\xi_1=\xi_2=1.995$, the number of iterations required is several orders of magnitude smaller than that for the method of Gerchberg-Papoulis. This improvement is of great practical importance when we want to design more complex images.

As mentioned in chapter 2 , for the case of coherent imaging, the input function f represents field distribution and as such is a complex function. By extending the class of inputs to include complex inputs as well, we hope to have better resolution.

Invoking the sampling theorem, to completely determine a real function $|\tilde{T}|$, band-limited to ω_0, we need $2\omega_0$ samples/sec. To represent a complex function $|\tilde{T}|e^{j\Omega\tilde{T}}$ which is band-limited to ω_1, we need $2\omega_1$ complex samples/sec or equivalently $4\omega_1$ real samples/sec. Therefore as long as ω_1 is not smaller than $\omega_0/2$, it may be possible to find a phase $\Omega\tilde{T}$ such that $|\tilde{T}|e^{j\Omega\tilde{T}}$ is band-limited to ω_1. For the two-dimensional case, a similar argument shows that ω_1 would have to be larger than $\omega_0/(2)^{1/2}$.

The above arguments show that it may indeed be possible to obtain better resolution using coherent imaging system with complex input and it provides limits on what we could hope to achieve. However, the problem of synthesis of the phase for a nonnegative function will lead itself to a nonconvex set problem (this is similar to the well known problem of recovering the phase from magnitude). The method proposed here cannot handle this problem and will not converge to the solution. An investigation of the alteration of this method or finding another algorithm is necessary for solving this problem.

Another constraint on the input function that is of great interest is the object itself being restricted to be of binary nature or to be quantized to a finite number of intensity levels. This restriction is very important, because of physical implementation considerations. Another example is computer holography [11] where the magnitude of the function is given and the coefficient of its Fourier Transform must be chosen from a set of quantized values (because of the limitations of the display device and the materials used to synthesize the hologram). However, the operation of quantizing a signal is not equivalent to projection onto a convex set, and therefore cannot be handled by this method. Further research is necessary to resolve this issue.

APPENDIX A

Definition 1

A DIFFRACTION-LIMITED optical imaging system is one which blocks the high frequency components of the input object.

Definition 2

A mapping $T:D\subset R^N\to R^N$ is nonexpansive on a set $D_0\subset D$ if

$$\left\|TX-TY\right\| \leq \left\|X-Y\right\| \qquad X,Y\varepsilon D_0 \ldots\ldots\ldots\ldots\ldots(1)$$

and strictly nonexpansive on D_0 if strictly inequality holds in (1) whenever $X\neq Y$.

Definition 3

A point X^* in the domain of T is called a fixed point of T if $TX^*=X^*$.

Definition 4

A sequence $\{f_n\}$ is said to converge strongly to f if

$$\lim_{n\to\infty}\left\|f_n-f\right\|=0$$

and is said to converge weakly to f if

$$\lim_{n\to\infty}(f_n,g)=(f,g)$$

for every $g\varepsilon R^N$, where (f,g) is the inner product operation of f and g. Note that strong convergence to f always implies weak convergence to f. In a finite-dimensional linear vector space, the converse is also true.

<u>Definition 5</u>

A subset D of R^N is said to be convex if, together with x_1 and x_2, it contains $\mu x_1+(1-\mu)x_2$ for all μ, $0\leq\mu\leq$. It is closed if it contains all its strong limit points.

<u>Definition 6</u>

A mapping $T:D\subset R^N\to R^N$ is said to be asymptotically regular if for every $x\varepsilon D$, $T^n x-T^{n+1}x\to 0$ as $n\to\infty$.

<u>Definition 7</u>

A mapping $T:D\subset R^N\to R^N$ is said to be a reasonable wanderer if for every $x\varepsilon D$,

$$\sum_{n=0}^{\infty}\left\|T^n x-T^{n+1}x\right\|^2<\infty.$$

It is evident that a reasonable wanderer is automatically asymtotically regular.

APPENDIX B

<u>Theorem 1</u> [2]

Let $P_c:R^N \to C$ is a operator projecting R^N onto C, $C \varepsilon R^N$ and such that

$$\left\| f-P_c f \right\| = \min \left\| f-x \right\| ,$$

where $f \varepsilon R^N$, then P_c is nonexpansive.

PROOF:

<u>Corollary 1</u> : Let C be a closed convex subset of R^N. Then for any $x \varepsilon R^N$

$$(x-P_c x, y-P_c x) \leq 0, \quad \text{all } y \varepsilon C. \quad \ldots\ldots\ldots\ldots\ldots\ldots (2)$$

In this guise it can be interpreted to mean that the vector $x-P_c x$ is supporting to C at the point $P_c x \varepsilon C$. As Figure A suggests, $x-P_c x$ is "normal" to the "tangent plane" to C erected at the point $P_c x$. This plane has C and x on opposite sides, and therefore seperates one from the other. Note also that the angle θ between the vectors $x-P_c x$ and $y-P_c y$ is never less than 90°.

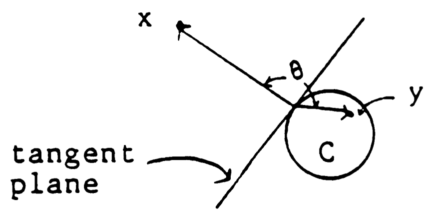

Figure A.

Corollary 2: Let C be any closed convex set. Then for every pair of elements x and y in R^N,

$$\left\| P_c x - P_c y \right\|^2 \leq (x-y, P_c x - P_c y). \quad \ldots\ldots\ldots\ldots\ldots (3)$$

proof: Since $P_c x$ and $P_c y$ both belong to C, it follows from (2) that

$$(x-P_c x, P_c y - P_c x) \leq 0 \ . \quad \ldots\ldots\ldots\ldots\ldots\ldots\ldots (4)$$

and

$$(y-P_c y, P_c x - P_c y) \leq 0, \ . \quad \ldots\ldots\ldots\ldots\ldots\ldots\ldots (5)$$

and (3) is obtained by addition of (4) and (5).

Now, Schwarz's inequality applied to (3), we will get, for every x and y in R^N,

$$\left\| P_c x - P_c y \right\| \leq \left\| x-y \right\| . \quad \ldots\ldots\ldots\ldots \quad (6)$$

Therefore, the operator P_c is nonexpansive.

Theorem 2 [2]

For $0 \le \xi_i \le 2$, the operator $T_i = 1 + \xi_i(P_i - 1) = (1-\xi_i) + \xi_i P_i$ is nonexpansive, where the operator P_i is nonexpansive.

Proof:

The assertion is obviously correct for $0 \le \xi_i \le 1$. For $1 < \xi_i \le 2$, it is found that, with the aid of (3) and (6),

$$\|T_i x - T_i y\|^2 = \|(1-\xi_i)(x-y) + \xi_i(P_i x - P_i y)\|^2 \quad \ldots\ldots (7)$$

$$= (1-\xi_i)^2\|x-y\|^2 + 2\xi_i(1-\xi_i)(x-y, P_i x - P_i y) + \xi_i^2\|P_i x - P_i y\|^2 \quad \ldots (8)$$

$$\le (1-\xi_i)^2\|x-y\|^2 + (\xi_i^2 + 2\xi_i(1-\xi_i))\|P_i x - P_i y\|^2 \quad \ldots\ldots (9)$$

$$= (1-\xi_i)^2\|x-y\|^2 + \xi_i(2-\xi_i)\|P_i x - P_i y\|^2 \quad \ldots\ldots (10)$$

$$\le (\xi_i(2-\xi_i) + (1-\xi_i)^2)\|x-y\|^2 = \|x-y\|^2 \quad \ldots\ldots (11)$$

and nonexpansive is established. Thus, $T = T_m T_{m-1} \ldots T_1$ is also nonexpansive.

Theorem A3 [17] Let $T: C \to C$ be an asymtotically regular nonexpansive operator with closed convex domain $C \subset H$, and let its set of fixed points $\Delta \subset C$ be nonempty. Then for $x \in C$, the sequence $\{T^n x\}$ is weakly convergent to an element of Δ. Moreover, the convergence is strong iff at least one subsequence of $\{T^n x\}$ converges strongly.

<u>Theorem</u> <u>3</u> [2]

The operator $T=T_m T_{m-1}.....T_1$ is a reasonable wanderer for $0<\xi_i<2$, $i=1\to m$.

proof:

For $m=1$, we have $T=T_1$, $C_0=C_1$ and

$$\|x-Tx\|^2=\xi_1{}^2\|x-P_1x\|^2. \quad ....(12)$$

Moreover, for any $y\varepsilon C_0$, $Ty=P_1y=y$ and

$$\begin{aligned}\|Tx-y\|^2&=\|x-y+\xi_1(P_1-x)\|^2 \quad ....(13)\\ &=\|x-y\|^2+2\xi_1(x-y,P_1x-x)+\xi_1{}^2\|x-P_1x\|^2 \quad ....(14)\\ &=\|x-y\|^2-\xi_1(2-\xi_1)\|x-P_1x\|^2+2\xi_1(x-P_1x,y-P_1x) \quad ....(15)\\ &\le\|x-y\|^2-\xi_1(2-\xi_1)\|x-P_1x\|^2 \quad ....(16)\end{aligned}$$

since the last term in (15) is nonpositive. Thus by combining (12) and (16), it is found that

$$\|x-Tx\|^2\le\xi_1(\|x-y\|^2-\|Tx-y\|^2)/(2-\xi_1) \quad ....(17)$$

for $0<\xi_1<2$.

For arbitrary $m\geq1$, a straightforward induction on m yields the inequality

$$\|x-Tx\|^2\le b_m.2^{m-1}(\|x-y\|^2-\|Tx-y\|^2) \quad ....(18)$$

where $y \varepsilon C_0$ and

$$b_m = \sup \left[\xi_i/(2-\xi_i)\right] .$$

(Clearly, (17) subsumes the case $m=1$.) In fact, let $T=T_mK$ where

$$K=T_{m-1}T_{m-2}\cdot\ldots\cdot T_1$$

and observe that for $m\geq 2$,

$$\begin{aligned}\|x-Tx\|^2 &= \|x-Kx+Kx-Tx\|^2 \\ &\leq (\|x-Kx\|+\|Kx-Tx\|)^2 \\ &\leq 2(\|x-Kx\|^2+\|Kx-Tx\|^2) \\ &\leq 2(\|x-Kx\|^2+2^{m-2}\|Kx-T_mKx\|^2). \quad \ldots\ldots\ldots\ldots\ldots\ldots(19)\end{aligned}$$

Thus, by induction hypothesis $((b_m\geq\xi_m)/(2-\xi_m)$ and $b_m\geq\sup_{1\leq i\leq m-1}\left[\xi_i/(2-\xi_i\right]$. Note also that $y\varepsilon C_0$ implies $y\ \ C_i$ and $y\varepsilon C_m$).

$$\begin{aligned}\|x-Tx\|^2 &\leq b_m.2(2^{m-2}\|x-y\|^2-2^{m-2}\|Kx-y\|^2+2^{m-2}\|Kx-y\|^2-2^{m-2}\|Tx-y\|^2) \\ &= b_m.2^{m-1}(\|x-y\|^2-\|Tx-y\|^2), \quad \ldots\ldots\ldots\ldots\ldots\ldots\ldots(20)\end{aligned}$$

the desired inequality. It now follows immediately from (20) that

$$\sum_{n=0}^{\infty} \|T^nx-T^{n+1}\|^2 \leq b_m 2^{m-1}\|x-y\|^2 < \infty,$$

and T is therefore a reasonable wanderer and, a fortiori, asymtotically regular. By Theorem A3, the sequence $\{T^n x\}$ converges weakly to a fixed point of T, and convergence is strong iff some subsequence converges strongly.

APPENDIX C

```
      DIMENSION IDM(64,64)
      COMPLEX ARRAY(64,64),CRRAY(64,64)
      DIMENSION BRRAY(64,64)
      ICOUNT=0
      KIND=1
      OPEN(5,FILE='SAW1')
      OPEN(6,FILE='ABC')
      CALL INITT(480)
      CALL DWINDO(0.,1536.,0.,1170.)
      CALL OPENTK('GSHADE',10)
      READ(5,15)M,NPOINT
15    FORMAT(2I2)
      DO 100 I=1,NPOINT
      READ(5,11)(IDM(I,J),J=1,NPOINT)
      DO 919 LI=1,NPOINT
919   IF(IDM(I,LI).EQ.0) IDM(I,LI)=-1
      DO 110 J=1,NPOINT
      ARRAY(I,J)=CMPLX(FLOAT(IDM(I,J)),0.0)
110   BRRAY(I,J)=REAL(ARRAY(I,J))
100   CONTINUE
11    FORMAT(64I1)
500   IND=0
      CALL FFT2D(ARRAY,M,KIND)
```

```
      CALL LPF(ARRAY,NPOINT)
      KIND=-KIND
      CALL FFT2D(ARRAY,M,KIND)
      IF(ICOUNT.EQ.0) THEN
        DO 901 NL=1,64
        DO 902 NP=1,64
          IF(REAL(ARRAY(NL,NP)).GE.0.0) THEN
          ARRAY(NL,NP)=(1.0,0.0)
          ELSE
           ARRAY(NL,NP)=(-1.,0.)
          ENDIF
902     CONTINUE
901     CONTINUE
        ELSEIF(ICOUNT.EQ.80) THEN
        WRITE(6,696)
696   FORMAT(15X,'     THE OUTPUT AFTER 80 ITERATION     ')
        ELSEIF(ICOUNT.EQ.300) THEN
        WRITE(6,299)
299     FORMAT(15X,'     THE OUTPUT AFTER 300 ITERATION     ')
        ELSEIF(ICOUNT.EQ.600) THEN
        WRITE(6,200)
200    FORMAT(15X,'     THE OUTPUT AFTER 600 ITERATION     ')
        STOP
      ENDIF
      CALL OVRF(ARRAY,BRRAY,NPOINT)
      CALL PROJ(ARRAY,IDM,NPOINT,IND)
```

```
      IF(IND.EQ.0) THEN
        DO 444 IT=1,NPOINT
        DO 444 JT=1,NPOINT
444     CRRAY(IT,JT)=ARRAY(IT,JT)
        KIND=1
        CALL FFT2D(CRRAY,M,KIND)
        CALL LPF(CRRAY,NPOINT)
        KIND=-KIND
        CALL FFT2D(CRRAY,M,KIND)
        CALL PROJ(CRRAY,IDM,NPOINT,IND)
        IF(IND.EQ.0) THEN
          WRITE(6,421) ICOUNT
421        FORMAT(15X,'    THE NUMBER OF ITERATION     =',I3)
          CALL QUN(ARRAY)
        CALL ANMODE
      CALL CLOSTK(10)
          STOP
        ENDIF
      ENDIF
      CALL OVRF(ARRAY,BRRAY,NPOINT)
      ICOUNT=ICOUNT+1
      KIND=-KIND
      GO TO 500
      END
```

```
      SUBROUTINE FFT2D(A,M,KIND)
      COMPLEX A(64,64),XX(64)
      IPOINT=2**M
      DO 50 IK=1,IPOINT
      DO 60 JK=1,IPOINT
60    XX(JK)=A(IK,JK)
      CALL FFT1D(XX,M,KIND)
      DO 70 JK=1,IPOINT
70    A(IK,JK)=XX(JK)
50    CONTINUE
      DO 71 JK=1,IPOINT
      DO 72 IK=1,IPOINT
72    XX(IK)=A(IK,JK)
      CALL FFT1D(XX,M,KIND)
      DO 73 IK=1,IPOINT
73    A(IK,JK)=XX(IK)
71    CONTINUE
      RETURN
      END
```

```
      SUBROUTINE LPF(B,NP)
      COMPLEX B(64,64)
      MPT=NP/2+1
      LWP=15
      KC=MPT-LWP
      KD=MPT+LWP
      LW=KC-1
      DO 113 LP=1,LW
      DO 114 KE=KC,KD
114   B(LP,KE)=(0.0,0.0)
113   CONTINUE
      DO 123 LE=KC,KD
      DO 125 LF=1,NP
125   B(LE,LF)=(0.0,0.0)
123   CONTINUE
      MC=KD+1
      DO 133 MM=MC,NP
      DO 135 NN=KC,KD
135   B(MM,NN)=(0.0,0.0)
133   CONTINUE
      RETURN
      END
```

```
      SUBROUTINE PROJ(AA,IBB,IP,IND)
      COMPLEX AA(64,64)
      DIMENSION IBB(64,64)
      PP=0.0010
      DO 333 I=1,IP
      DO 433 J=1,IP
      T=REAL(AA(I,J))
      IF((ABS(T)-PP).LT.-0.00001) THEN
         T=FLOAT(IBB(I,J))*PP
         AA(I,J)=CMPLX(T,0.0)
         IND=1
          ELSEIF((T*FLOAT(IBB(I,J))).LT.0.0) THEN
           T=FLOAT(IBB(I,J))*PP
           AA(I,J)=CMPLX(T,0.0)
           IND=1
      ENDIF
433   CONTINUE
333   CONTINUE
      RETURN
      END
```

```
      SUBROUTINE FFT1D(X,M,KIND)
      COMPLEX X(64),U,W,TT
      N=2**M
      PI=3.14159265358979
      IF(KIND.EQ.1) GO TO 9
      DO 8 IL=1,N
8     X(IL)=CONJG(X(IL))/FLOAT(N)
9     DO 20 L=1,M
      LE=2**(M+1-L)
      LE1=LE/2
      U=(1.0,0.0)
      W=CMPLX(COS(PI/FLOAT(LE1)),-SIN(PI/FLOAT(LE1)))
      DO 20 J=1,LE1
      DO 10 I=J,N,LE
      IP=I+LE1
      TT=X(I)+X(IP)
      X(IP)=(X(I)-X(IP))*U
10    X(I)=TT
20    U=U*W
      NV2=N/2
      NM1=N-1
      J=1
      DO 30 I=1,NM1
      IF(I.GE.J) GO TO 25
      TT=X(J)
      X(J)=X(I)
```

```
      X(I)=TT
25    K=NV2
26    IF(K.GE.J) GO TO 30
      J=J-K
      K=K/2
      GO TO 26
30    J=J+K
      IF(KIND.EQ.1) RETURN
      DO 863 I1=1,N
863   X(I1)=CONJG(X(I1))
      RETURN
      END
```

```
      SUBROUTINE OVRF(ARR,BRR,NPT)
      COMPLEX ARR(64,64)
      DIMENSION BRR(64,64)
      RAN=1.995
      DO 37 L1=1,NPT
      DO 47 L2=1,NPT
      TAT=(1.-RAN)*BRR(L1,L2)+RAN*REAL(ARR(L1,L2))
      ARR(L1,L2)=CMPLX(TAT,0.0)
      BRR(L1,L2)=TAT
47    CONTINUE
37    CONTINUE
      RETURN
      END
```

```
      SUBROUTINE QUN(QA)
      COMPLEX QA(64,64)
      DIMENSION IAA(0:10),ICC(-10:0),IDD(64,64)
      READ(5,27)IAA
27    FORMAT(8I1,3I1)
      READ(5,27)ICC
      DO 633 I=1,64
      DO 733 J=1,64
      TP=REAL(QA(I,J))
      IF(TP.GT.1.0) THEN
        IDD(I,J)=9
        ELSEIF(TP.GT.0.0) THEN
        MP=TP*10.0
        IDD(I,J)=IAA(MP)
        ELSEIF(TP.LT.-1.0) THEN
        IDD(I,J)=0
        ELSE
        MP=TP*10.0
        IDD(I,J)=ICC(MP)
      ENDIF
733   CONTINUE
633   CONTINUE
      DO 827 I=1,64
      WRITE(6,927)(IDD(I,J),J=1,64)
827   CONTINUE
927   FORMAT(1X,64I1)
```

```
CALL SHADE(IDD)
RETURN
END
```

```
      SUBROUTINE PRINT(BL)
      COMPLEX BL(32,32)
      CHARACTER CA(96,96),BCC(98),AS,BS
      DO 677 I=1,32
      DO 777 J=1,32
      TM=REAL(BL(I,J))
      I1=I*3-2
      J1=J*3-2
      I2=I*3
      J2=J*3
      IF(TM.GE.0.0) THEN
        DO 877 II=I1,I2
        DO 877 JJ=J1,J2
877     CA(II,JJ)='W'
        ELSE
        DO 977 II=I1,I2
        DO 977 JJ=J1,J2
977     CA(II,JJ)=' '
      ENDIF
777   CONTINUE
677   CONTINUE
      WRITE(6,988)
988   FORMAT(////15X,'     THE OUTPUT IMAGE     ')
      DO 676 I=1,98
676   BCC(I)='*'
      AS='*'
```

```
      BS='*'
      WRITE(6,545)(BCC(I),I=1,98)
545   FORMAT(1X,98A1)
      DO 656 I=1,96
656   WRITE(6,545)AS,(CA(I,J),J=1,96),BS
      WRITE(6,545)(BCC(I),I=1,98)
      RETURN
      END
```

```
      SUBROUTINE SHADE(M)
      DIMENSION  M(64,64)
      CALL NEWPAG
      DO 1 I=0,1152,1152
      X=I
      CALL MOVEA(X,0.)
      CALL DRAWA(X,1152.)
1     CONTINUE
      DO 2 J=0,1152,1152
      Y=J
      CALL MOVEA(0.,Y)
      CALL DRAWA(1152.,Y)
2     CONTINUE
      DO 10 IR=1,64
      DO 20 IC=1,64
      IMG=M(IR,IC)
      IF(IMG.EQ.0) GOTO 20
      XMIN=18*(IC-1)
      XMAX=18*IC
      YMIN=1152-18*IR
      YMAX=1152-18*(IR-1)
      CALL MOVEA(XMAX,YMAX)
      CALL DRAWA(XMIN,YMIN)
      IF(IMG.EQ.1) GO TO 20
      DO 30 J=1,IMG
      CALL MOVEA(XMIN+(XMAX-XMIN)*J/(IMG),YMAX)
```

```
      CALL DRAWA(XMIN,YMAX-(YMAX-YMIN)*J/(IMG))
      CALL MOVEA(XMAX,YMAX-(YMAX-YMIN)*J/(IMG))
      CALL DRAWA(XMIN+(XMAX-XMIN)*J/(IMG),YMIN)
30    CONTINUE
20    CONTINUE
10    CONTINUE
      RETURN
      END
```

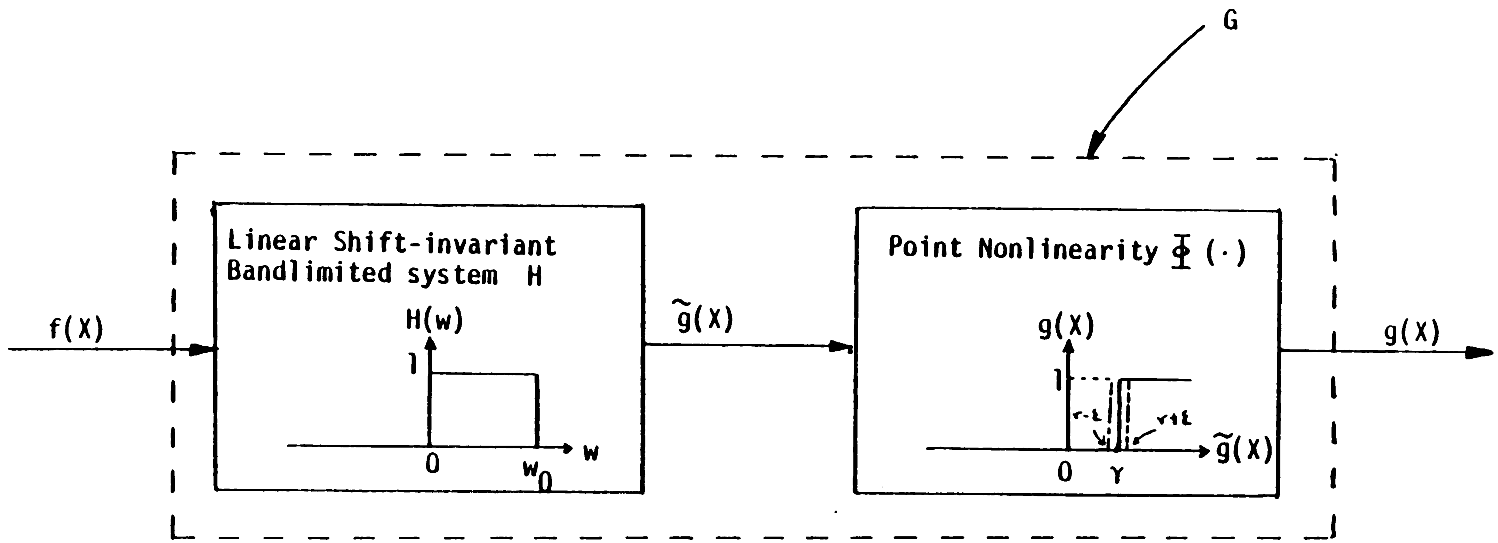

Figure 2.1 Incoherent imaging system

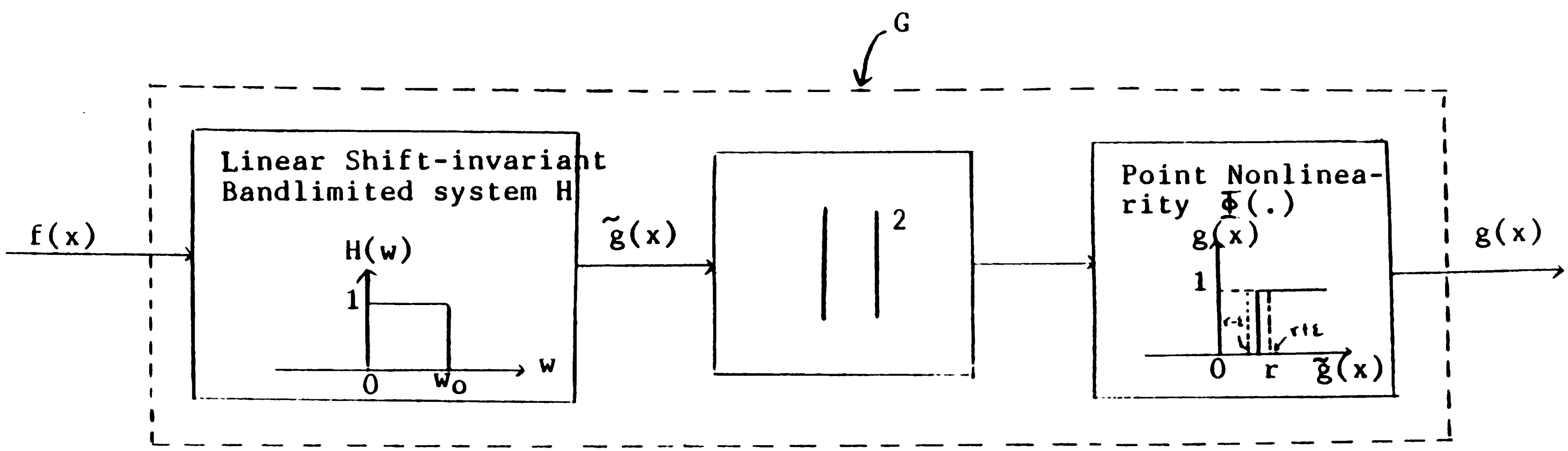

Figure 2.2 Coherent imaging system

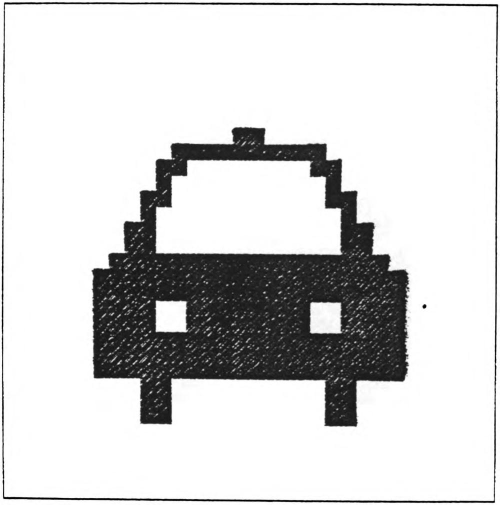

Figure 3a. Desired Pattern (Pattern 1)

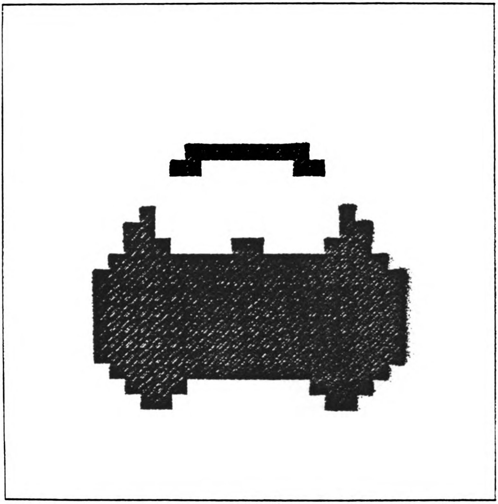

Figure 3b. Constructed pattern when the object in Figure 3a. is used as an input to the imaging system in Figure 2.1.

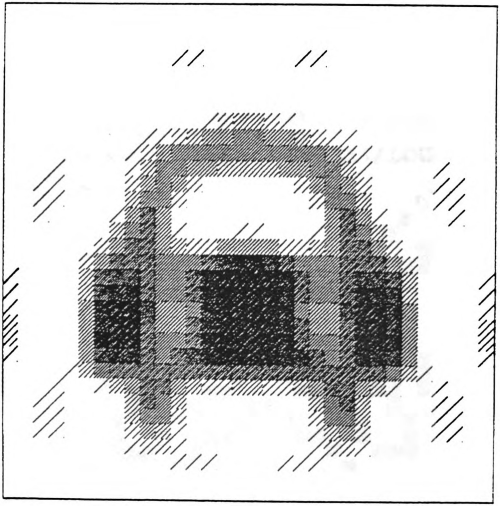

Figure 3c. Input pattern found by our iterative procedure which has been quantized into 10 gray levels.

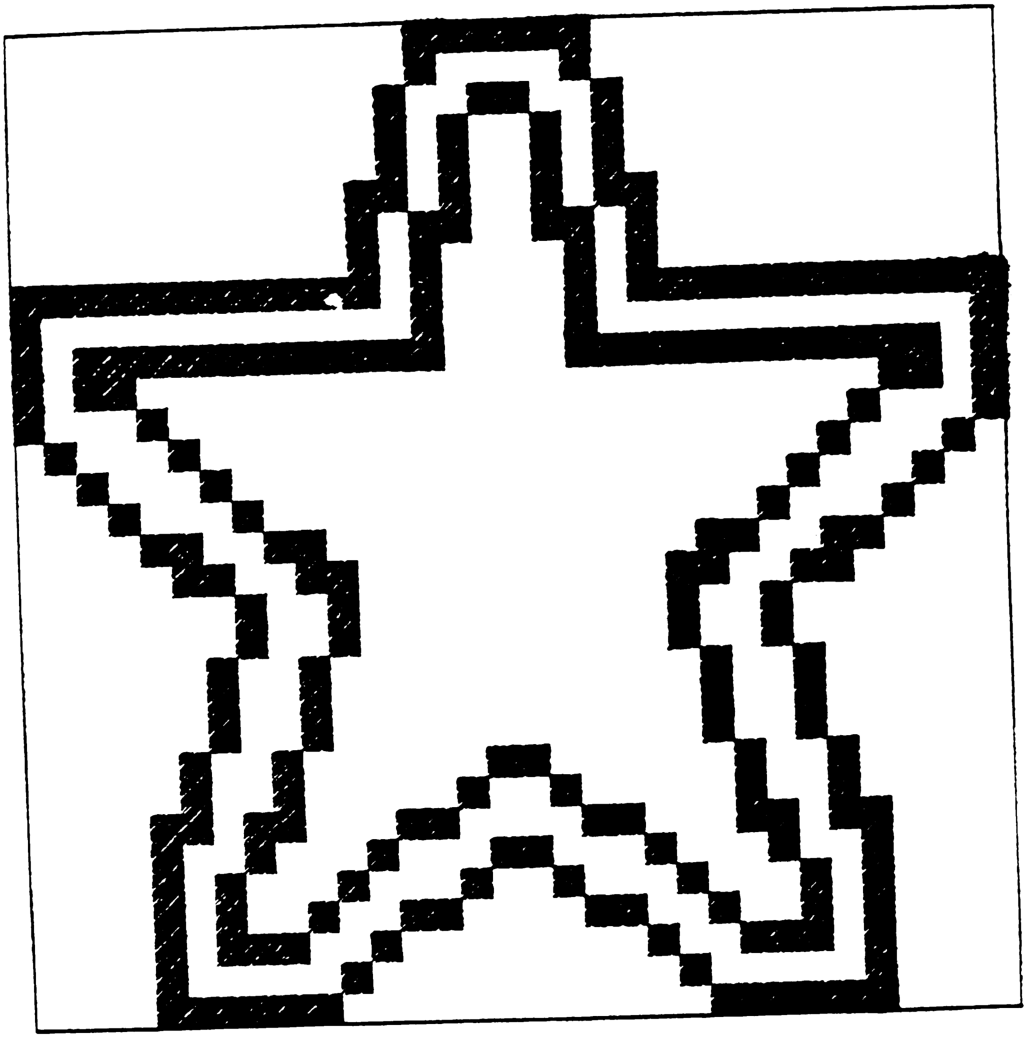

Figure 4a. (Pattern 2)

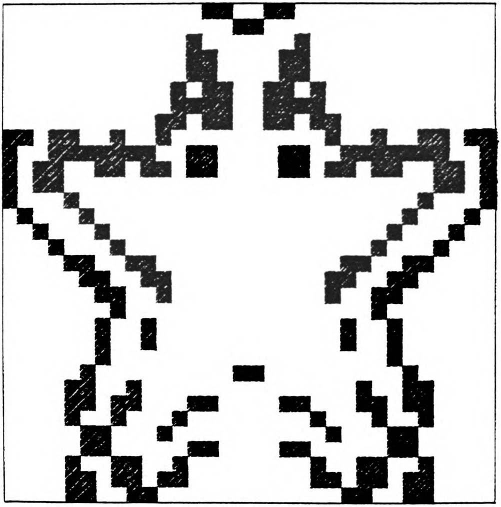

Figure 4b.

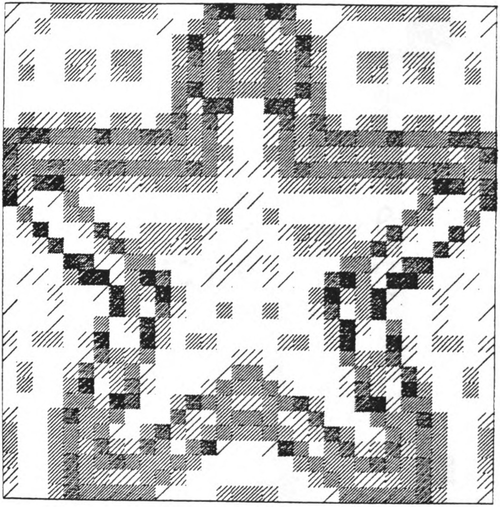

Figure 4c.

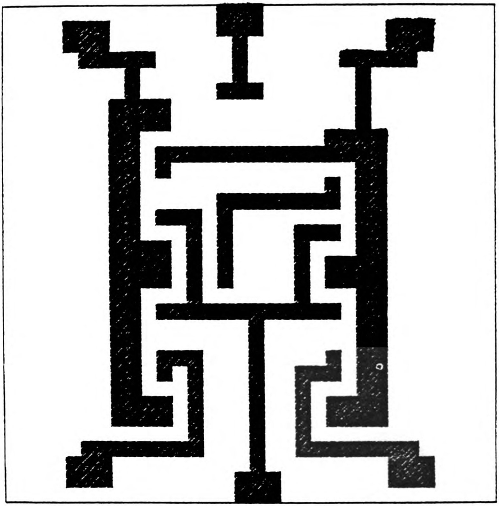

Figure 5a. (Pattern 3)

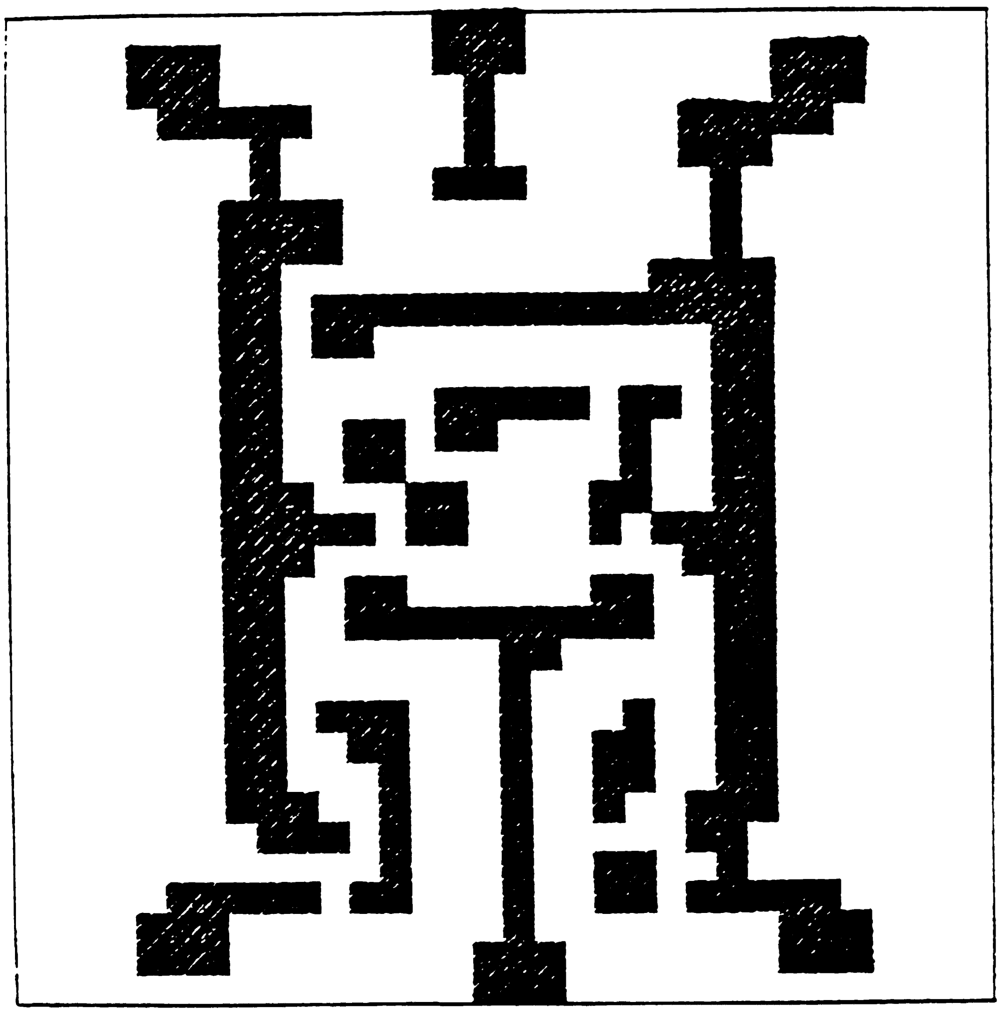

Figure 5b.

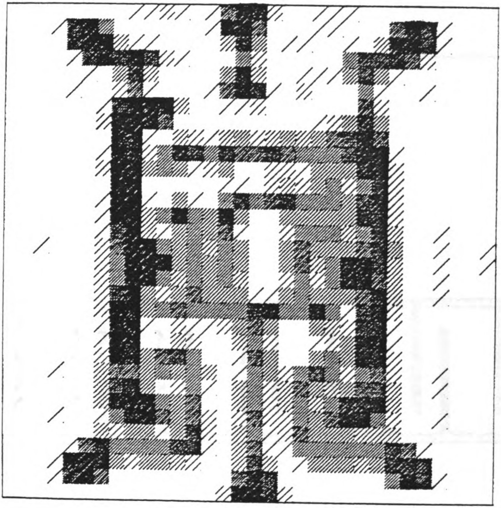

Figure 5c.

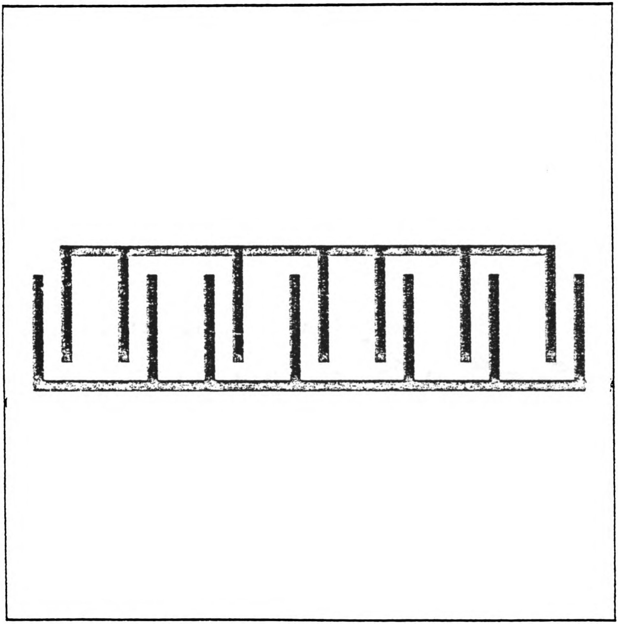

Figure 6a. (Pattern 4) Surface acoustic wave device

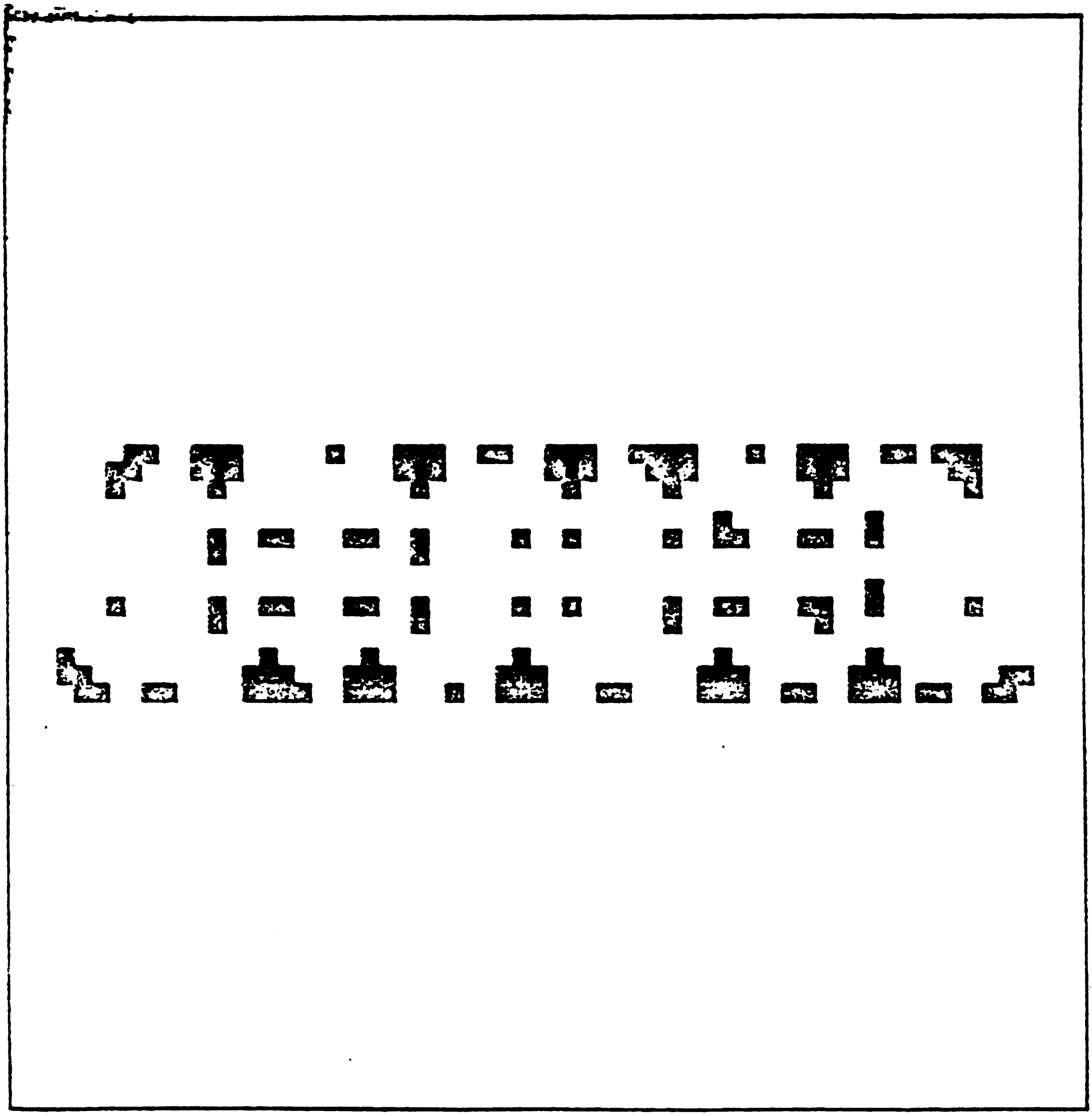

Figure 6b.

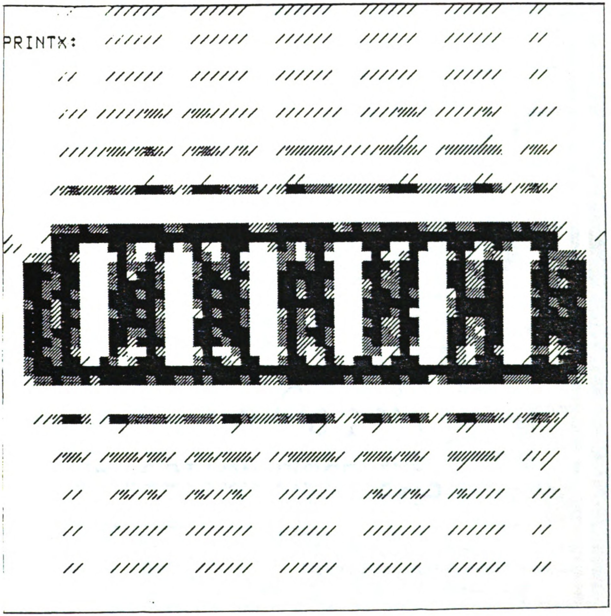

Figure 6c.

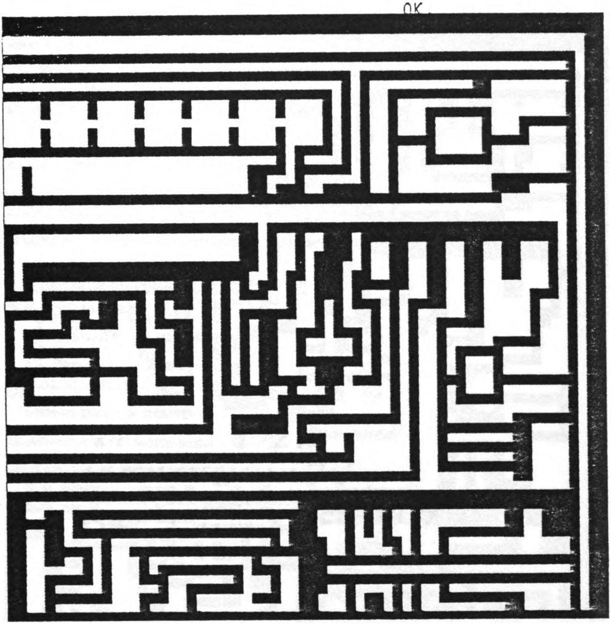

Figure 7a. (Pattern 5) Mask for microlithography in IC fabrication process.

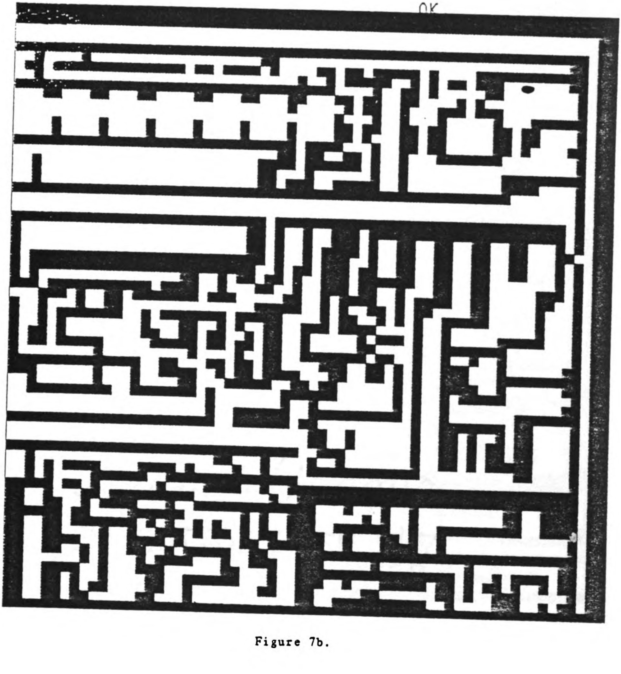

Figure 7b.

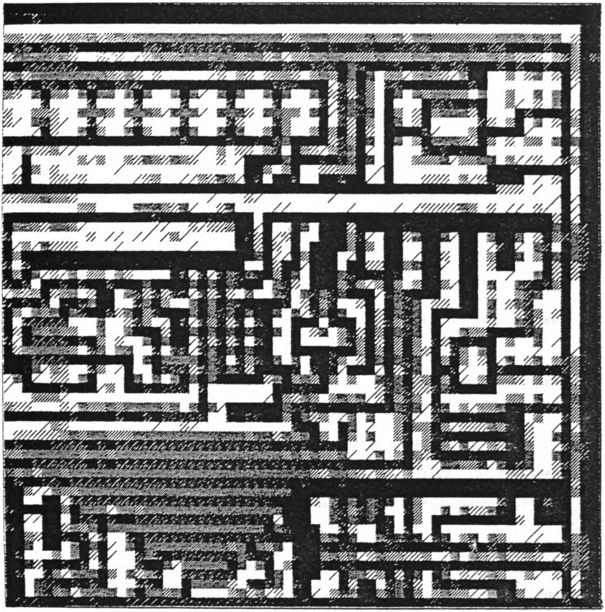

Figure 7c.

REFERENCES

[1] Y. Kok. Synthesis of images through a diffraction-limited system with high contrast recording, M.S. thesis, Michigan State University, E. Lansing, 1983.

[2] D.C. Youla and H. Webb, Image restoration by the method of convex projections: Part I-Theory, IEEE Trans. on Medical Imaging, Vol. MI-1, pp. 81-94, 1982.

[3] B.E.A. Saleh and S.I. Sayegh, Reduction of errors of microphotographic reproductions by optimal corrections of original mask, Opt. Eng., Vol. 20, pp. 781-784, Sept. 1981.

[4] Eastman Kodak Co., Techniques of microphotography. Publications No. P-52, Rochester, New York, 1967.

[5] G.W.W. Stevens, MIcrophotography, Butler and Tanner, London, 1968.

[6] S.I. Sayegh, B.E.A. Saleh and K.M. Nashold, Image design: Generation of prescribed image through a diffraction-limited system with high contrast recording, to be published.

[7] S.I. Sayegh, Image restoration and image design in nonlinear optical system, Ph.D. thesis, University of Wisconsin, Madison, 1982.

[8] A. Papoulis, A new algorithm in spectral analysis and bandlimited extrapolation, IEEE Trans. Circuits and Syst., Vol. CAS-22, PP. 735-742, 1975.

[9] J.R. Fienup, Iterative method applied to image reconstruction and to computer-generated hologram, Opt. Eng., Vol. 19, pp. 297-305, 1980.

[10] A.V. Oppenheim and J.S. Lim, The importance of phase in signals, Proc. IEEE, Vol. 69, pp. 529-541, 1981.

[11] R.A. Gabel and B. Liu, Minimization of reconstruction error with computer-generated binary hologram, Appl. Opt. Vol. 9, pp. 1180-1190, 1970.

[12] N.C. Gallagher and B. Liu, Method for computing kinoforms that reduces image reconstruction error, Appl. Opt., Vol. 12, pp. 2328-2335, 1973.

[13] R.S. Elliot, Synthesis of rectangular planer arrays for sum patterns with ring side lobes of arbitrary topography, Radio Science, Vol. 12, pp. 653-657, 1977.

[14] L.R. Rabiner, Linear program design of finite impulse response (FIR) digital filters, IEEE Trans. on Audio and Electroacoustic, Vol. Au-20, pp. 280-288, 1972.

[15] J. Goodman, Introduction to Fourier Optics, McGraw-Hill, 1968.

[16] N.I. Akhiezer and I.M. Glazman, Theory of linear operators in Hilbert space, Vol. 1, New York: Ungar, 1978.

[17] D.C. Youla, Image restoration by the method of projections onto convex sets-Part 1, POLY-MRI 1420-81, Dec. 1981.